Crop Protection 209 (2026) 107776

Contents lists available at ScienceDirect

Crop Protection

journal homepage: www.elsevier.com/locate/cropro

Research article

Environmental, resident and bystander exposure from spraying applications with unmanned aerial vehicles equipped with flat-fan nozzles or rotary atomizers

Pierre-Henri Dubuis [a], Céline Villars-Corbex [a], M. Clare Butler Ellis [b], H. Christoph Geiser [c], Jeremy J. Harwood [b], Marco C. Knobloch [c], Andrew G. Lane [b], Aurélie Melgar [a], Joel D. Stohler [d], Clive R. Tuck [b], Helen C. Wheeler [b], Jürg A. Zarn [c,1], Sebastian L.B. König [c,*]

[a] Agroscope, Swiss Federal Agricultural Research Station in Changins, Nyon, 1260, Switzerland
[b] Silsoe Spray Applications Unit, Wrest Park, Silsoe, Bedford, MK45 4HP, United Kingdom
[c] Federal Food Safety and Veterinary Office (FSVO), Toxicology of Plant Protection Products, Bern, 3003, Switzerland
[d] Agroscope, Electronic Support, Zurich, 8046, Switzerland

A B S T R A C T

Adoption of agricultural unmanned aerial vehicles (UAVs) for spraying plant protection products has proceeded at a rapid pace. A trend towards usage of UAV sprayers fitted with rotary atomizers has been noted. Regarding the risks associated with UAV-based plant protection treatments, the existing body of literature on environmental and resident/bystander exposure primarily relates, however, to UAVs equipped with hydraulic nozzles. Rotary atomizers and hydraulic nozzles are different in how they produce spray. The possible influence of the delivery system on the risks posed by UAV sprayers was therefore assessed in several laboratory and field experiments relating to a reference UAV sprayer fitted with hydraulic flat-fan nozzles as well as two UAV sprayers equipped with rotary atomizers. Droplet measurements revealed similar volumes of drift-prone droplets for a given $D_{V0.5}$ independent of the delivery system. Considering the results of spray pattern experiments and other relevant aspects, swath widths of 3.0–4.5 m were chosen in drift and exposure trials. Drift and resident/bystander exposure generally decreased at increasing distance from the edge of the target area and at increasing height above the ground. Crosswind and droplet size rather than the delivery system were identified as primary drivers of off-target droplet movement.

1. Introduction

Adoption of agricultural unmanned aerial vehicles (UAVs) for spraying plant protection products has proceeded at a rapid pace, especially in East Asia (Bonds et al., 2024). Many commercial UAV sprayers are fitted with hydraulic nozzles, such as flat-fan nozzles or hollow-cone nozzles. However, numerous recently released UAV platforms use rotary atomizers as delivery systems. In fact, 70 % of UAV sprayers used in China have been reported to use rotary atomizers (Wang et al., 2023b). A trend towards usage of UAV sprayers fitted with rotary atomizers has also been noted in Switzerland (Anken et al., 2025).

Rotary atomizers achieve atomization *via* spinning discs, which are typically characterized by radial grooves and pins at the edges (Chen et al., 2022). Spray liquid delivered onto these spinning discs is ejected horizontally as droplets (Chen et al., 2022). It has been reported that rotary atomizers built into UAV sprayers can generate spray droplets with diameters ranging from approximately 85–550 μm depending on the disc rotation rate (Wang et al., 2023b). Moreover, they are suitable for low-volume and variable-rate spraying and do not clog frequently (Wang et al., 2023b). Considering the ejection of spray liquid in the horizontal plane, it has been hypothesized that UAVs equipped with rotary atomizers may be associated with significant drift risk (Chen et al., 2022; Wang et al., 2020). Indeed, it has been shown in wind tunnel experiments that for a given $D_{V0.5}$, droplets produced by rotary atomizers were more prone to drift than those generated by hydraulic nozzles used as a reference (Wang et al., 2023b). Here, the $D_{V0.5}$ is where 50 % of the total spray volume consists of droplets of equal or lesser diameter (OECD, 2021).

The U.S. Environmental Protection Agency (US EPA) defines drift as "the movement of pesticide dust or droplets through the air at the time

* Corresponding author.
E-mail address: sebastian.koenig@blv.admin.ch (S.L.B. König).
1 Retired.

https://doi.org/10.1016/j.cropro.2026.107776
Received 14 February 2026; Received in revised form 30 June 2026; Accepted 16 July 2026
Available online 16 July 2026

of application or soon after, to any site other than the area intended" (US EPA, 2026). Drift can affect the environment, such as wildlife and water bodies, and people's health, for example, when individuals not involved in agricultural operations ("residents", "bystanders") are exposed (EFSA, 2022; US EPA, 2026). In aerial applications, drift may be influenced by environmental factors (e.g., crosswind speed and direction, relative humidity, air temperature), aircraft-specific parameters (e.g., induced airflow, release position of the spray relative to aircraft-induced airflow) and operational parameters (e.g., droplet size/velocity spectra generated by the nozzles/atomizers, release position over the target) (Zhang et al., 2023).

A dedicated standard of the International Organization for Standardization (ISO) exists for measuring deposition of spray drift onto horizontal surfaces and airborne drift (ISO 22866, 2005). Numerous studies characterizing the drift risk of UAV sprayers have been conducted accordingly. Some of these studies involved low crops or a surrogate thereof, such as (artificial) rice, (shredded) corn, wheat, weeds and stubble (Ahmad et al., 2022; Butler Ellis et al., 2026; Chen et al., 2020; Goulet-Fortin et al., 2024; Herbst et al., 2020; Huang et al., 2023a; Wang et al., 2018, 2020; Xue et al., 2014). Further studies were done in high crops or a surrogate thereof, such as (artificial) vine, apple and olive (Brown and Giles, 2018; Dubuis et al., 2023; Liu et al., 2020; Psiroukis et al., 2026; Sánchez-Fernández et al., 2023, 2024; Wang et al., 2021, 2023a). However, only 5 out of the 17 studies referenced above have been performed with UAV sprayers equipped with rotary atomizers (Butler Ellis et al., 2026; Goulet-Fortin et al., 2024; Liu et al., 2020; Wang et al., 2020; Xue et al., 2014).

The OECD has recently identified a need for generating more data on exposure associated with UAV sprayer technology (OECD, 2021). A few studies on resident/bystander exposure have been published in the meantime: Dubuis et al. (2023) evaluated resident/bystander exposure *via* the dermal and the inhalation route following applications in an apple orchard. Gao and co-workers quantified the dermal exposure of residents/bystanders following treatments of bare soil, a soybean plot and a peach orchard (Gao et al., 2025). The dermal exposure of residents/bystanders was also the focus of field trials performed in a vineyard (Sánchez-Fernández et al., 2025) and a coconut plantation (Lan et al., 2024), respectively. However, only one of these studies was done with a UAV sprayer fitted with rotary atomizers (Lan et al., 2024).

The objective of this study was to assess environmental, resident and bystander exposure resulting from plant protection treatments with a reference UAV sprayer fitted with hydraulic flat-fan nozzles as well as two UAV sprayers equipped with rotary atomizers to elucidate the possible influence of the delivery system on the risks posed by UAV sprayers. For this purpose, the droplet size distributions produced by different flat-fan nozzles and the rotary atomizers mounted onto the UAVs were characterized. Subsequently, spray pattern measurements were conducted. The results of these experiments as well as other relevant aspects were considered to define the distance between two neighboring spray tracks ("swath width") in drift and exposure trials. The latter consisted of a total of 12 drift trials designed to meet the requirements of the corresponding ISO standard (ISO 22866, 2005). In these trials, direct dermal and inhalation exposure of residents and bystanders to spray drift was also characterized.

2. Material and methods

2.1. Application equipment

Three UAV sprayers were selected: The DJI Agras T30 and T50 (both Da-Jiang Innovations Science and Technology Co., Ltd, Shenzhen) and the XAG P100 Pro (XAG Co., Ltd., Guangzhou). All three UAV sprayers are electrical-powered and similar regarding size. They can also achieve similar flight precision in the satellite-assisted autopilot mode. However, there are differences regarding the delivery systems. In particular, the T30 is fitted with 16 hydraulic nozzles, while the other two UAV sprayers each have built-in rotary atomizers. Further differences relate to the number and relative arrangement of the rotors, the nozzle/atomizer layout and the tank volume. Technical specifications are summarized in Table 1. In all field trials, the T30 and T50 were operated by DigitalRoots SA (Granges, Switzerland) and the P100 Pro was piloted by Sky53 sagl (Chiasso, Switzerland), both of which are agricultural service providers.

2.2. Spray liquid

Except for some of the droplet size measurements that were performed with tap water (Table 2), experiments were performed with 0.3 % v/v Helios 500 SC and 0.02 % w/v Etalfix Pro (both products: Syngenta Crop Protection AG, Basel, Switzerland) in tap water. Helios 500 SC is a suspension concentrate that contains the fluorescent tracer 2,5-thiophenediylbis(5-tert-butyl-1,3-benzoxazole) at a nominal concentration of 500 g/L. Etalfix Pro is a wetting agent. The same combination of tracer and wetting agent has been used in earlier trials (Dubuis et al., 2023).

2.3. Droplet size characterization

All droplet size measurements were performed by the Silsoe Spray Applications Unit (Bedford, United Kingdom).

2.3.1. Spray generated by rotary atomizers

The rotary atomizers built into the T50 and the P100 Pro were tested for droplet size at different flow rates and disc speeds using either tap water or the tank mix described in Section 2.2 (Table 2). Here, the aim was to comply with the requirements of ISO 25358:2018 as closely as possible (ISO 25358, 2018). The experimental setup is depicted in Fig. 1. Briefly, the UAV sprayer to be tested was mounted on a custom-built fixed frame located inside a wind tunnel. Rotors were not operating during the experiments and no crosswind was applied. Measurements were performed at 17 °C. A Visisizer (Oxford Lasers Ltd., Didcot, United Kingdom) was used as a measurement system for droplet size. The system permits to detect particles that are 21.5–2039 μm in diameter. A laser was used to illuminate the region of interest from behind and shadow images of the subject were taken with a digital camera. The laser and camera were triggered so that a single laser pulse froze the motion of the subject during each frame capture. The use of the technique for agricultural sprays has been published (Murphy et al., 2001). The instrument was operated in spatial mode, *i.e.*, snapshots of droplets captured within the sample volume were taken. The detection volume was placed 1100 mm below the nozzle. At this distance, droplets are expected to fall vertically and the Visisizer optical lens is not vulnerable to contamination by the spray. To account for the dispersion at the sampling distance chosen, the Visisizer optical bench was mounted on rollers so it could be moved over 2400 mm from the center of the disc outwards for each of the required disc speeds and pump rates. Two (tap water) or three (diluted tracer) replicate measurements were made for each setting.

2.3.2. Spray produced by flat fan nozzles

Three flat-fan nozzles were used and operated as indicated in Table 2. Measurements were made using the tank mix described in Section 2.2, which was at a temperature of 16 °C. They involved a Spraytec laser diffraction system (Malvern Panalytical Ltd., Malvern, United Kingdom), which allows for detection of particles that are 8.3–1025 μm in diameter. Standard protocols for spray classification according to ISO 25358:2018 were used (ISO 25358, 2018). Briefly, spatial data were recorded in single scans to sample the complete spray plume 350 mm below the nozzle. Ambient temperatures were 17–18 °C. Three replicate measurements were acquired for each setting.

Table 1
Technical specifications of the UAV sprayers used.

	DJI Agras T30	DJI Agras T50	XAG P100 Pro
Type	Hexacopter with single rotors	Coaxial quadcopter	Quadcopter with single rotors
UAV length × width × height, unfolded including blades	2858 mm × 2685 mm × 790 mm	2800 mm × 3085 mm × 820 mm	2927 mm × 2868 mm × 725 mm
Propeller diameter	965 mm	1372 mm	1397 mm
Empty weight with batteries	36.5 kg	52.0 kg	54.0 kg
Tank volume	30 L	40 L	50 L
Minimal horizontal and vertical hovering precision (real-time kinematic positioning enabled)	±10 cm	±10 cm	±10 cm
Nozzle/atomizer number and type	16 Teejet XR 11001 VK flat spray nozzles[a]	2 built-in rotary atomizers	2 built-in rotary atomizers
Spraying angle	110°	180°	180°
Nozzle/atomizer layout	Within the respective rotor diameters	Within the respective rotor diameters	Directly under the respective rotor axes

[a] During all field trials, the 4 nozzles at the leading edge of the aircraft were consistently turned off. Hence, only 12 nozzles were operating simultaneously. This was an automatic adjustment made by default by the control software. Teejet XR 11001 VK nozzles were selected from a total of three flat fan nozzles assessed for droplet size (see Section 2.3.2).

Table 2
Spray parameters assessed in the droplet size measurements.

Spray liquid	Nozzle/ atomizer	Pressure (bar)	Flow rate (L/min/nozzle or atomizer)	Droplet sizes or rotation rates selected in the control software
Helios 500 SC and Etalfix Pro, diluted in tap water	Teejet XR11002	0.65	0.366	-
	Teejet XR110015	1.15	0.367	-
	Teejet XR11001	2.40	0.366	-
	T50	-	3.6	100–400 µm
	T50	-	2.2	100–400 µm
	P100 Pro	-	3.6	3300–10,000 min^{-1}
	P100 Pro	-	2.2	2500–7000 min^{-1}
Tap water	T50	-	3.6	100–500 µm
	P100 Pro	-	3.6	3300–10,000 min^{-1}
	P100 Pro	-	2.2	2500–7000 min^{-1}

2.4. Spray pattern measurements

The trial site for spray pattern measurements was in Sierre, Switzerland (46.272029° N, 7.489275° E). It consisted of lawn growing on a flat field at an elevation of ~512 m above sea level. All trials involved the equipment described in Section 2.1 and the spray liquid containing Helios 500 SC and Etalfix Pro described in Section 2.2. They were performed on May 9, 2024 (P100 Pro), June 25, 2024 (T30 and T50), and November 27, 2024 (T30).

The following steps were performed with the UAV sprayers on the ground: Sprayer tanks were fully loaded. The flow rate was set to 0.36 L/min/nozzle or 2.2 L/min/atomizer. Nominal droplet sizes were set for the UAV sprayers fitted with rotary atomizers, which was a requirement of the respective UAV control software (T50: 170 µm, P100 Pro: 150 µm). The target flight speed and flight height were 6.0 m/s and 3 m, respectively. During the trials conducted on June 25, 2024, the T30 was set to a flight speed of 2.9 m/s. This was a deviation from the study plan (Section 3.1).

The trial layout is depicted in Fig. 2. It is largely based on an approach reported elsewhere (Li et al., 2021). Briefly, wooden planks were placed in lines perpendicular to the flight line, forming three transects. The total width of each transect was 8 m. Adjacent transects were spaced 7 m apart. 40 Petri dishes with a diameter of 8.8 cm (Fischer Scientific, Reinach, Switzerland) were fixed onto each transect using double-sided sticky tape. The distance between the centers of two neighboring Petri dishes was 20 cm. The flight trajectory corresponded to a straight line passing through the center of each transect that was followed in the autopilot mode. Spraying began at least 70 m before reaching the first transect and continued for at least 70 m beyond the last transect. Each trial was replicated twice, *i.e.*, 2 × 3 transects were sampled. Based on anemometer measurements conducted on-site, crosswind speeds were <0.3 m/s at a height of 2.4 m above the ground during all trials. All samples were collected, transported to Agroscope, Changins, Switzerland, and stored in the dark at ambient temperature until further analysis (Section 2.6).

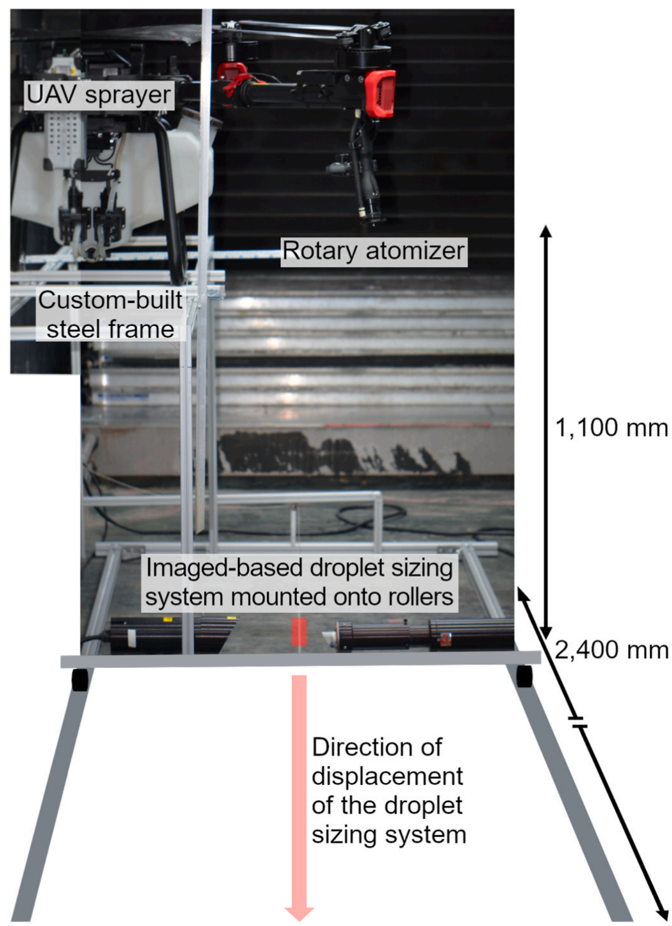

Fig. 1. Setup to characterize the spray produced by rotary atomizers. The figure consists of two merged photographs and additional annotations.

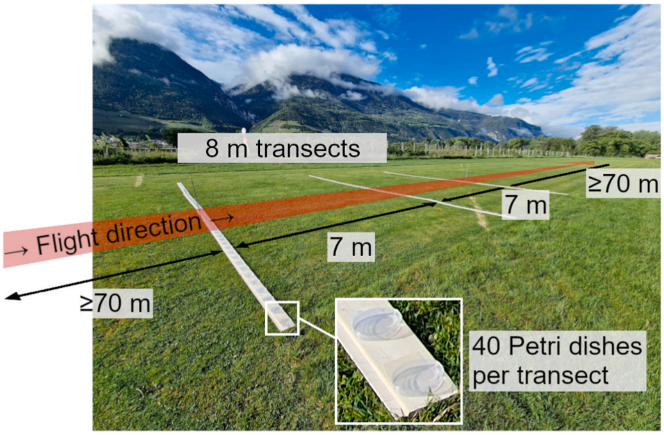

Fig. 2. Annotated photograph of the experimental setup used for spray pattern measurements.

2.5. Drift and exposure trials

The methodology was largely based on that of an earlier study (Dubuis et al., 2023).

2.5.1. Trial sites

Drift and exposure trials were conducted at two sites. Site 1 was in Collombey-Muraz, Switzerland (46.281456° N, 6.938675° E), at an elevation of ~387 m above sea level. It corresponded to a field with a ~1.6 % slope containing barley stubble. A corn field was located ~50 m upwind of the target area for spraying. Within ~100 m of the target area, there were other agricultural fields containing cereal stubble and an agricultural road. Site 2 was in Vouvry, Switzerland (46.332759° N, 6.923252° E). The elevation was ~382 m above sea level and the slope ~1.7 %. The plot contained recently cut alfalfa with a maximum plant height of 5 cm. An agricultural road was located within 20 m. A plot with low vegetables and a hedge were located next to the detection area ~50 m downwind of the target area.

Table 3
Spray applications performed within the context of the drift and exposure trials.

Application/trial no.	Date	Local time (CET)	Site	UAV sprayer
1	Jul 9, 2024	From 10:27 a.m. onward	Collombey-Muraz	P 100 Pro
2	Jul 9, 2024	From 11:59 a.m. onward	Collombey-Muraz	P 100 Pro
3	Jul 11, 2024	From 10.31 a.m. onward	Collombey-Muraz	T50
4	Jul 11, 2024	From 11.45 a.m. onward	Collombey-Muraz	T50
5	Jul 11, 2024	From 12.59 a.m. onward	Collombey-Muraz	T50
6	Sep 17, 2024	From 12:22 a.m. onward	Vouvry	P 100 Pro
7	Sep 17, 2024	From 13:58 a.m. onward	Vouvry	P 100 Pro
8	Sep 18, 2024	From 11:24 a.m. onward	Vouvry	T30
9	Sep 18, 2024	From 12:21 a.m. onward	Vouvry	T30
10	Sep 19, 2024	From 11:07 a.m. onward	Vouvry	T30
11	Sep 19, 2024	From 12:03 a.m. onward	Vouvry	T30
12	Sep 20, 2024	From 10:13 a.m. onward	Vouvry	T50

2.5.2. Applications

Spray applications were performed as described in Table 3. The following steps were performed with the UAV sprayers on the ground: (i) The flow rate of the nozzles/atomizers was tested before the first trial of the day (Glass, 2006). For this purpose, the T30 was set to a nominal flow rate of 0.5 L/min/nozzle and the actual output over 60 s was collected. For the other UAV sprayers, a nominal flow rate of 2.2 L/min/atomizer and a collection time of 30 s were used. The measured volumetric output generally deviated from the target output by 4 % or less for all nozzles/atomizers except for a single measurement, where the deviation was 8 %. (ii) The spraying system was flushed with spray liquid for roughly 5 s to remove undesired residues (before each application). (iii) A sample from the spray liquid was taken directly from a nozzle/atomizer (before and after each application). These samples were used to determine actual tracer concentrations (Section 3.4.2).

Target application parameters were identical to those used in spray pattern measurements (Section 2.4) apart from the flow rate of the T30, which was set to 0.41 L/min/nozzle. Considering the swath widths (Sections 2.5.3 and 3.3), nominal spray volumes were 30.4 L/ha (T30), 27.2 L/ha (T50) and 40.7 L/ha (P100 Pro), respectively.

2.5.3. Trial layout

The trial layout was designed to meet the requirements of ISO 22866:2005. It was identical at both trial sites. As shown in Fig. 3, the target area for spraying was 100 m long. It was sprayed in a back-and-forth pattern in autopilot mode. Based on the rationale provided in Section 3.3, the distance between two neighboring spray tracks ("swath width") was set to 4.5 m (T30, T50) or 3.0 m (P100 Pro). The width of the target area was 22.5 m (T30, T50) or 21.0 m (P100 Pro), which corresponds to 5 (T30 and T50) or 7 spray tracks (P100 Pro), respectively. The edge of the target area was defined as half a swath from the downwind spray track (OECD, 2021). Airborne spray was measured 5 m downwind. Sedimented spray droplets were collected inside the target area and 0, 1, 3, 5, 10, 15, 20, 30 and 50 m downwind. Three display mannequin pairs, each representing an adult and a child resident/bystander spaced by ~1 m, were placed 5 m and 15 m downwind, respectively. 4 further mannequin pairs were positioned at a downwind distance of 10 m. Mannequin pairs were distributed in a staggered manner over the different downwind distances to minimize "shadowing" effects. All mannequins located 5 m downwind as well as 2 adult and 2 child mannequins located 10 m downwind were equipped with personal air sampling pumps.

2.5.4. Collectors

Photographs of the collectors used are shown in Fig. 3. Airborne drift at different heights was assessed with a 6 m tall sampling tower with three vertical polyester strings (diameter = 2 mm, Meister & Cie AG Rüegsau, Rüegsauschachen, Switzerland). Sedimented spray droplets were collected with a total of 20 Petri dishes per distance (diameter = 8.8 cm, Fischer Scientific, Reinach, Switzerland), which corresponds to a combined collector area of 1216 cm^2 per distance. Resident/bystander exposure to spray drift was quantified based on the whole body method and the personal sampling method (OECD, 1997). Display mannequins measuring 175 cm or 110 cm in height were used to represent adults or children, respectively. Adult mannequins were dressed in loose fit medium size coveralls that served as dermal dosimeters. For child mannequins, small size adult coveralls with shortened arms and legs were used (both coverall types: 3M-4570, 3M, Saint Paul, MN, USA). 5 adult mannequins and 5 child mannequins were further equipped with personal air-sampling pumps (Sensidyne, LP, St. Petersburg, FL, USA) to draw air from the breathing zone. Here, cotton wool was used as collector material for spray droplets.

2.5.5. Meteorological monitoring

A weather station (Campbell Scientific, Logan, UT, USA) was used to record the air temperature and the relative humidity at a height of 2 m.

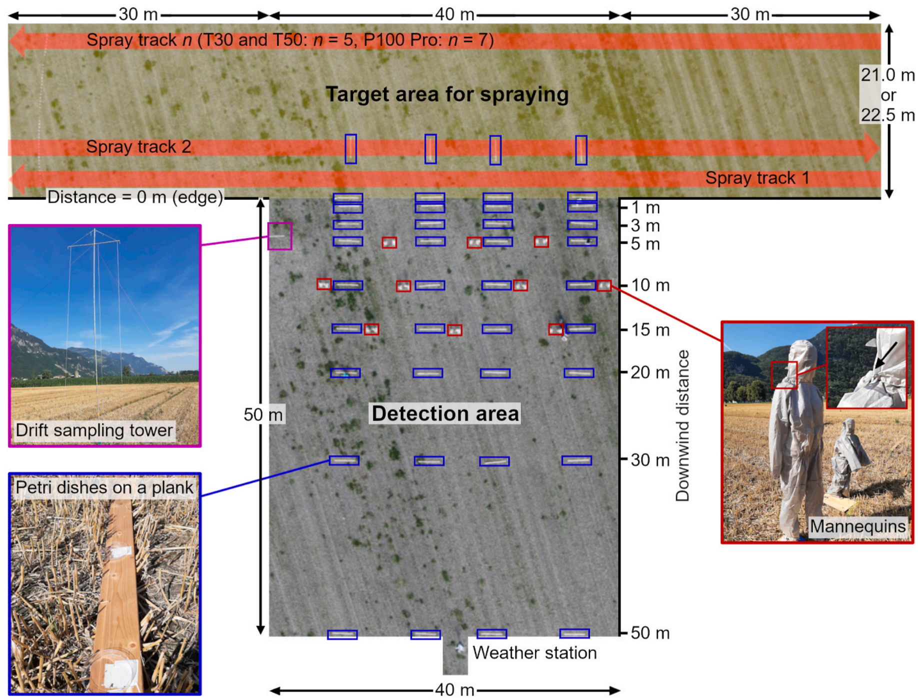

Fig. 3. Layout of the drift and exposure trials. The figure consists of an annotated aerial photograph of trial site 2. Spray tracks 1 and 2 as well as the last spray track are represented with red arrows. The location of the different collectors is highlighted: blue = Petri dishes on a plank, magenta = drift sampling tower, red = a pair of display mannequins (child, adult). Photographs of the collector systems that were taken at trial site 1 are also included. The inset figure on the righthand side shows the inlet of the rubber tube attached to the personal air-sampling pump. The inlet is further highlighted with an arrow. (For interpretation of the references to colour in this figure legend, the reader is referred to the Web version of this article.)

In addition, crosswind speed and direction were measured at a height of 3 m using an anemometer (Gill Instruments Limited, Hampshire, United Kingdom). All data were recorded at a frequency of 0.5 Hz at a downwind distance of ~53 m (Fig. 3).

2.5.6. *Trial conduct*

At the beginning of each trial day, 10 × 4 planks and 10 × 2 wooden bases were placed at their pre-defined positions relative to the edge of the target area. Personal air sampling pumps were set to a flow rate of 5 L/min. The anemometer and the weather station were also set up.

Prior to each application, polyester strings were attached to the upper end of the sampling tower, followed by setting up the tower and securing the strings using pegs. 5 Petri dishes were fixed onto each plank using double-sided sticky tape. The distance between adjacent Petri dishes was roughly 0.5 m. Mannequins were dressed and fixed onto the wooden bases. A rubber tube was attached to the inlet of each pump and the other end fitted with cotton wool (50 mg ± 1 mg per sampling train). Subsequently, the cotton-filled end was clamped to the side of the headpiece of the coverall worn by the respective mannequin. Care was taken to avoid any contamination of the collector material due to contact with the ground.

The spray liquid was prepared 10–20 min before the first application of each trial day using an opaque mixing vessel with a total volume of ~120 L located at the edge of the trial site. To maintain homogeneity, the spray liquid was regularly stirred. Shortly before each application, the UAV sprayer tank was filled with spray liquid to 100 % of its nominal value. At the end of each application, the spray liquid remaining in the tank was transferred back to the mixing vessel. Unless necessary for mixing, loading and unloading, the mixing vessel was kept closed.

During suitable crosswind conditions, the sampling pumps were switched on, followed by sprayer actuation. The sampling period ended 4 min after the end of the spraying application. Similar waiting times were used in earlier trials (Dubuis et al., 2023; Fritz and Martin, 2020). Subsequently, personal air sampling pumps were switched off, followed by sample collection (Section 2.5.7).

On September 17–20, 2024, a total of 56 field recovery samples were prepared to quantify possible loss of tracer. Please refer to the Supplementary Methods for further details.

2.5.7. *Sample collection*

Samples were collected within 30 min or less. To avoid contamination, disposable nitrile gloves (Gillingham, United Kingdom) were worn and regularly changed during the procedure. Polyester strings were cut into six sections from the ground upwards (~1 m per section). Each section was placed into a pre-labeled Falcon tube (Fischer Scientific AG, Reinach, Switzerland), which was then closed. Petri dishes were closed, pooled per distance and each pooled sample was wrapped using a pre-labeled plastic bag. Coverall parts covering head, torso (chest and back including upper thigh groin level), upper limbs and lower limbs were collected separately and wrapped using pre-labeled bags (OECD, 1997). Cotton wool filters were collected individually and placed into pre-labeled Falcon tubes (Fischer Scientific AG, Reinach, Switzerland), which were then closed.

2.5.8. *Sample transport and storage*

All samples were shipped to Agroscope, Changins, Switzerland, and stored in the dark at ambient temperature until further analysis.

2.6. *Analytical tracer quantification*

The analytical method was largely based on that reported by Dubuis et al. (2023). Briefly, tracer was recovered from Petri dishes by adding 10 mL of 2-propanol, followed by incubation on a rotary plate for at least 15 min. 40 mL of 2-propanol were added to tubes containing sections of polyester string from the sampling tower while 10 mL of 2-propanol were added to tubes with cotton wool filters. Subsequently, tubes were vortexed for 2 min. Finally, coverall parts stored in individual plastic bags were soaked thoroughly in 150 mL (head) or 300 mL of

2-propanol (other body parts) for at least 10 min. Solvents at 99.6 % ACS for extraction were purchased from Acros Organics.

After extraction, tracer material was quantified fluorometrically (λ_{ex} = 375 nm, λ_{em} = 435 nm, Fluorimeter 96, Syngenta Crop Protection AG, Basel, Switzerland). The instrument was calibrated regularly (~20 times) with unformulated tracer dissolved in 2-propanol over the course of the analytical phase of the study. The lower limit of quantification (LLOQ) was at 1 μg/L, which corresponds to the following amounts of tracer per sample considering the solvent volumes used for extraction:

- Petri dishes, cotton wool filters: 0.01 μg
- Sections of polyester string: 0.04 μg
- Coverall parts covering the head: 0.15 μg
- Coverall parts covering upper limbs, torso or lower limbs: 0.30 μg

If necessary for achieving a signal within the linearity range of the fluorimeter, sample solutions were further diluted with 2-propanol. Please refer to the Supplementary Methods for details on the validation of the analytical method.

2.7. Data analysis

RStudio (R ver. 4.3.2) was used, including the libraries *ggplot2* ver. 3.5.1 (Wickham, 2016), *ggpubr* ver. 0.6.0 (Kassambara, 2025) and *MASS* ver. 7.3-60 (Venables and Ripley, 2002).

2.7.1. Droplet data

Volume diameters, $D_{V0.1}$, $D_{V0.5}$ and $D_{V0.9}$, were calculated. They define where 10/50/90 % of the total spray volume consists of droplets of equal or lesser diameter (OECD, 2021). Relative spans were computed as follows:

$$relative\ span = \frac{D_{V0.9} - D_{V0.1}}{D_{V0.5}} \quad (1)$$

The proportion of spray volume contained in droplets with diameters below 100 μm was also calculated.

2.7.2. Spray pattern data

Measured deposition values were used to explore the relationship between swath width and deposition uniformity as described (Li et al., 2021). Briefly, the results obtained from the three transects were averaged together for each replicate. Each averaged distribution was used to generate copies thereof that were then overlaid with an offset. Here, the offset represents the swath width, which was varied. With respect to the T50 and the P100 Pro, adjacent copies were also reversed to account for the 180° aircraft rotation that occurs between two neighboring spray tracks. These overlays simulate the depositions patterns achieved in back-and-forth flight mode. An 8-m-snapshot from each overlay was used to compute the respective coefficient of variation. The effective swath width was determined from the mean coefficients of variation found in any of the replicates.

2.7.3. Airborne drift, ground deposition and exposure data

3 airborne drift samples, 68 ground deposition samples and 8 inhalation exposure samples were characterized by residue levels below the respective LLOQ. They were set to ½ LLOQ.

Ground deposition and airborne drift data as well as exposure data were analyzed as described (Dubuis et al., 2023): Ground deposition and airborne drift values were normalized to the respective actual application rate (OECD, 2021). Height-dependent mean airborne drift and distance-dependent mean ground deposition values were computed. Ground deposition data were further used to calculate cumulative projections (ISO 22866, 2005) as well as 50th, 77th, 90th and 95th inclusive percentiles at a given downwind distance. Measurements involving personal air-sampling pumps attached to mannequins were corrected for differences between the flow rate of the pump and the actual inhalation rate of a person (EFSA, 2022). To calculate exposure percentiles from the distribution of dermal or inhalation exposure measurements in the sample, adult or child exposure data were combined as indicated in Section 3.4.5 and fitted to a log-normal probability density function:

$$f(x) = \frac{1}{x\sigma\sqrt{2\pi}} \exp\left(-\frac{(\ln(x) - \mu)^2}{2\sigma^2}\right) \quad (2)$$

where x denotes the exposure expressed as a volume of spray liquid, μ is the location parameter and σ corresponds to the scale parameter. The respective cumulative distribution functions were used to derive 50th, 75th and 95th percentiles.

Based on the same combined datasets, 75th and 95th percentiles were also estimated statistically:

$$percentile\ estimate = \exp\left(\bar{x} + t_{n-1,\alpha} \cdot s \cdot \sqrt{1 + \frac{1}{n}}\right) \quad (3)$$

Here, $\bar{x}$ and s are the arithmetic mean and the standard deviation of the natural logarithms of the exposure measurements, respectively, n denotes the sample size and $t_{n-1,\alpha}$ is the 75th or 95th percentile of the t-distribution for the respective α value and n-1 degrees of freedom (EFSA, 2022). Computing percentiles from the distribution of exposure measurements and *via* statistical estimation and using the higher of the two values has been recommended by the European Food Safety Authority (EFSA, 2022).

3. Results

3.1. Deviations from the study plan

The following unexpected events occurred:

a) In the spray pattern experiments performed with the P100 Pro on May 9, 2024, 37 out of 240 Petri dishes were blown off the planks.
b) The spray pattern trials involving the T30 conducted on June 25, 2024, were performed at a flight speed of 2.9 m/s instead of 6.0 m/s.
c) In drift and exposure trial 3, the outermost 20 m of spray track 4 and all of spray track 5 were not sprayed due to low battery. Please refer to Fig. 3 for further information on the spray tracks concerned.
d) In drift and exposure trials 6 and 7, the width of the target area was 19 m instead of 21 m, and hence, the size of the target area was 0.19 ha instead of 0.21 ha. Inspection of the data logs revealed that spray tracks 1–6 were regularly spaced by 3 m as intended. In turn, tracks 6 and 7 were spaced by approximately 1.5 m. According to the operator, the reduced swath width was likely automatically accounted for by spraying the last track with only one atomizer instead of two.
e) In all drift and exposure trials combined, 18 out of 2400 Petri dishes were blown off the planks and 8 out of 240 adult mannequins toppled over backwards during the sampling period.

These deviations were dealt with as follows:

a) The Petri dishes concerned were excluded from further analysis.
b) The experiment was replicated twice on November 27, 2024, at the intended flight speed of 6.0 m/s. Only one valid replicate was obtained.
c) Even though the requirements regarding the width of the treated area were not fulfilled (ISO 22866, 2005), it should be emphasized that >90 % of deposition outside the target area was confined within a downwind distance of less than 10 m (Section 3.4.4). No further measures were taken.
d) Despite the deviation, the actual spray volume was in excellent agreement with the target value (Section 3.4.2). Also, >90 % of deposition outside the target area was confined within a downwind

distance of less than 5 m (Section 3.4.4). No further measures were taken.

e) The Petri dishes concerned were excluded from further analysis. Compared to other adult mannequins located at the same downwind distances, the mannequins that had toppled over were not characterized by unexpectedly high or low exposure values (data not shown). Data from these mannequins were therefore not excluded.

3.2. Droplet size distributions

Droplet data were acquired before conducting the spray pattern experiments (Section 3.3) and the drift and exposure trials (Section 3.4). These data were used to determine rotary atomizer settings for subsequent field trials and to select the flat-fan nozzles to be used in conjunction with the T30. Measurements of rotary atomizers were done with complete systems in stationary mode without the rotors operating. In this mode, disc rotation rates could be directly set in the control software of the P100 Pro. In turn, the software of the T50 permitted to indirectly control this parameter by setting a target droplet size. The results are summarized in Supplementary Table S1 (tap water) and Supplementary Table S2 (0.3 % Helios 500 SC + 0.02 % Etalfix Pro). In general, higher rotation rates increased the proportion of fine droplets. For a given target rotation rate/target droplet size and UAV sprayer, the proportion of fine droplets was somewhat higher at the lower of the two flow rates tested, *i.e.*, 2.2 L/atomizer. Regarding the T50, differences between set droplet sizes and measured $D_{V0.5}$ values were noted. For both rotary atomizers, the relationship between the set droplet size or the set rotation rate and the measured $D_{V0.5}$ and %V < 100 µm values relating to diluted tracer could be empirically described with power functions (Supplementary Fig. S1). Three flat-fan nozzles were also assessed (Supplementary Table S2).

Based on the results of the droplet measurements and the nominal application parameters (Sections 2.4 and 2.5.2), the actual spray characteristics in the spray pattern experiments and the drift and exposure trials were estimated:

- T30 fitted with Teejet XR 11001 VK nozzles: $D_{V0.5}$ = 166 µm, %V < 100 µm = 18.43 %
- T50: $D_{V0.5}$ = 136 µm, %V < 100 µm = 22.94 %

It should be noted that the T30 was set to a flow rate of 0.405 L/min/nozzle in the context of the drift and exposure trials. This required a calculated pressure of 2.56 bar. This altered the droplet spectrum of the nozzles ($D_{V0.5}$ = 130 µm, %V < 100 µm ~ 40 %, Simon Caldwell and Daniel Schneider, Syngenta Crop Protection, personal communication). Based on the published literature, the estimated spray qualities were considered representative of UAV-based non-herbicidal treatments of low crops (Huang et al., 2023b; Shan et al., 2022; Wang et al., 2019, 2023c).

For applications in dynamic flight mode, the control software of the P100 Pro required a nominal droplet size to be selected (here: 150 µm). A control experiment involving a custom-built tachometer was performed to identify the disc speed corresponding to the nominal droplet size, and thus, allow for an estimation of the actual spray characteristics (Supplementary Methods). This experiment was done retrospectively after the spray pattern and drift and exposure trials. The estimated spray characteristics were:

- P100 Pro: $D_{V0.5}$ = 238 µm, %V < 100 µm = 6.17 %

The estimated $D_{V0.5}$ is greater than the selected droplet size.

3.3. Spray pattern analysis

Spray pattern data were acquired for parameter selection in the drift and exposure trials. Positional adjustment to account for any displacement of the plume due to wind differences, a correction performed in other studies (Fritz and Martin, 2020), was not performed here because ambient wind speeds were low. Tracer levels were averaged for each distance from the flight center line, UAV sprayer and flight speed. At a flight speed of 6.0 m/s, the largest tracer amounts were consistently recovered from Petri dishes that were close to the flight center line (Fig. 4A, C, E). At the outermost sampling distances, mean residue levels were ~40 % (T30), ~25 % (T50) and <5 % (P100 Pro) of the respective maximum. The total averaged tracer amounts recovered followed the order P100 Pro > T50 > T30. Overall, this indicates that the UAV sprayers tested, especially the T30 and T50, might project a considerable amount of spray liquid beyond the sampled area under the experimental conditions. For future trials, it is therefore recommended to increase the width of the sampled area. For the T30 flying at 2.9 m/s, the transversal deposition profile was bimodal and asymmetric (Fig. 4G).

The relationship between swath width and deposition uniformity under back-and-forth flight mode was explored (Fig. 4B, D, F, H). In general, coefficients of variation increased at greater swath widths. From these data, effective swath widths (ESWs) were determined. The Swiss regulatory framework for UAV sprayers defines the ESW as the largest swath width with a coefficient of variation below 15 % (Anken et al., 2025). As this threshold relates to stationary measurements without forward component (OECD, 2021), it was relaxed to 20 % in the present study. The fact that the control software packages allowed for adjusting swath widths in discrete steps was also considered. ESWs were 5.0 m (T30, 6.0 m/s), 4.5 m (T30, 2.9 m/s), 5.5 m (T50) and 2.5 m (P100 Pro). On average, 68 % (T30, 6.0 m/s), 79 % (T30, 2.9 m/s), 82 % (T50) and 59 % (P100 Pro) of the total amount of spray recovered were found within these ESWs.

The above-mentioned ESWs were considered for selecting swath widths in the drift and exposure trials. Regarding the T30, the results of the spray pattern experiments conducted at a flight speed of 2.9 m/s had to be used, as the experiments at a flight speed of 6.0 m/s had not yet been performed at the time the swath widths had to be defined. It has recently been recognized that other criteria than uniformity can be important when setting swath widths (Castro-Tenzi et al., 2025; Fritz and Martin, 2020). In the present study, the following additional criteria were considered: (i) The experimental layout of the drift and exposure trials (Fig. 3) and the definition of the edge of the target area (Section 2.5.3) imply that a decrease in swath width shifts spray tracks closer to the detection area. Low albeit realistic swath widths are therefore best suited to yield a representative worst-case estimate of drift and exposure. (ii) It was considered unlikely that any of the three UAV sprayers would be operated at a swath width of less than 3.0 m in practice. Thus, it was decided to set swath widths to 4.5 m (T30 and T50), and 3.0 m (P100 Pro). Comparable swath widths have been chosen in other drift trials (Ahrens et al., 2025; Butler Ellis et al., 2026; Herbst et al., 2020; Wang et al., 2020).

3.4. Drift and exposure trials

3.4.1. Meteorological conditions

Environmental conditions, which can affect the drift risk, were monitored downwind the target area for spraying during the drift and exposure trials. All meteorological data are summarized in Supplementary Table S3. Briefly, mean dry and wet bulb temperatures during the trials were 15.3–27.2 °C and 12.6–21.9 °C, respectively. Differences between dry and wet bulb temperatures greater than 8 °C, which have previously been associated with rapid droplet shrinkage and high drift risk (Zhang et al., 2023), were not noted. Mean crosswind speeds ranged from 1.2 to 5.1 m/s during spraying operations. None of the trials were characterized by conditions typically associated with surface temperature inversions, such as little to no wind and dark ground surface (Portillo et al., 2025; Zhang et al., 2023). Mean crosswind directions were generally close to the perpendicular of the spray

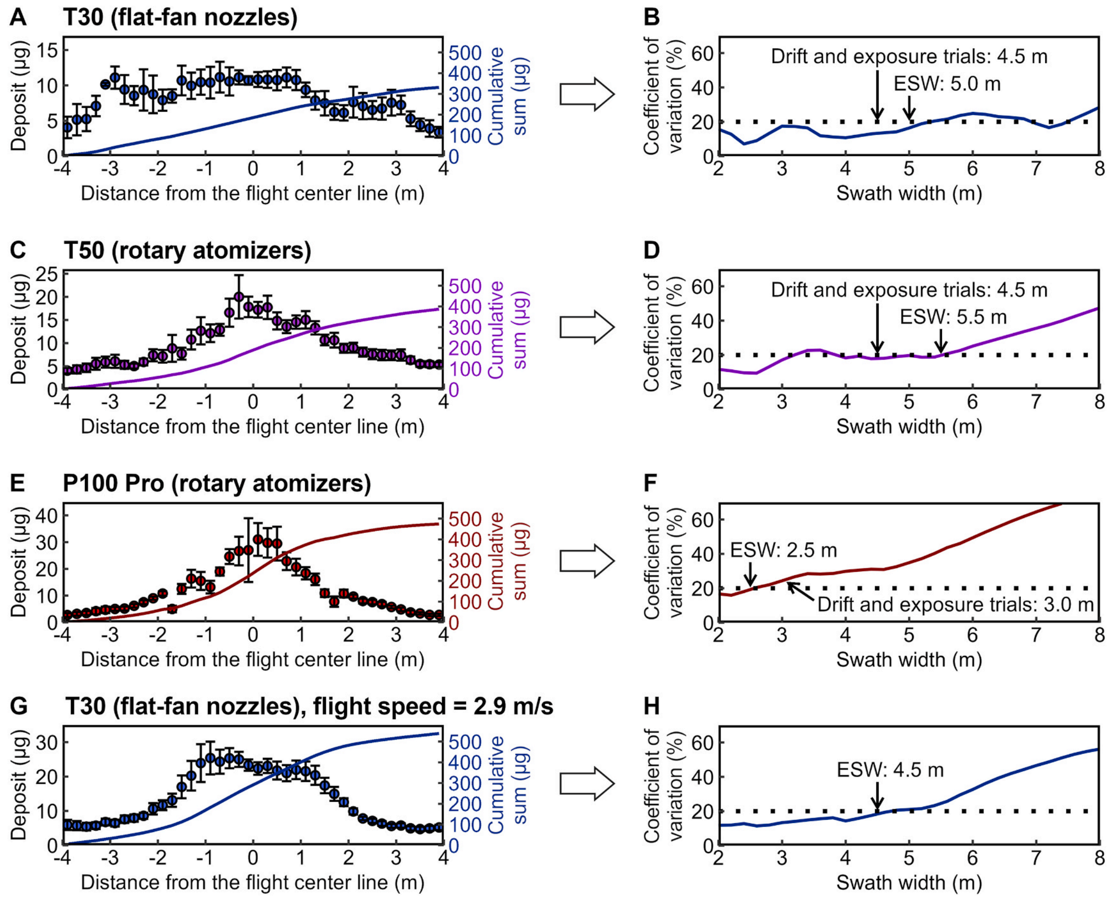

Fig. 4. Analysis of spray pattern data. A-H. Results of trials involving the T30, T50 or P100 Pro, respectively. Panels on the left depict spray patterns that were averaged over all replicates (circles) as well as the corresponding standard errors (error bars) and cumulative sums (solid lines). Panels on the right show the relationship between swath width and the estimated deposition uniformity under back-and-forth flight mode (solid lines). Dotted lines indicate the threshold that was employed to determine ESWs. The latter are indicated with arrows in addition to the swath widths chosen in the drift and exposure trials.

track but less so during trials 1, 3, 6 and 8. The wind conditions during these four trials did not fully comply with the acceptance criteria defined in the ISO standard (Supplementary Table S3) (ISO 22866, 2005).

3.4.2. *Tracer concentration, application rates, field recoveries*

Averaged measured tracer concentrations ranged from 1.37 to 1.81 g/L. This range matches the nominal tracer concentration of 1.50 g/L well. For each trial, the actual spray volume [L/ha] was calculated from the applied volume [L] and the sprayed area [ha] taken from the respective data log. Actual spray volumes were 29.3–29.5 L/ha (T30), 27.3–30.7 L/ha (T50), and 39.9–40.3 L/ha (P100 Pro). These values hardly deviate from the nominal spray volumes of 30.4 L/ha (T30), 27.2 L/ha (T50), and 40.7 L/ha (P100 Pro). Actual tracer concentrations and actual spray volumes were used to calculate airborne drift, ground deposition and exposure values.

Four field recovery samples showed different recoveries than the other samples and were therefore considered outliers. Marginal amounts of fluorescent material were recovered from blank samples (0–0.75 µg per collector). The overall recoveries from fortified samples excluding outliers were:

- Petri dishes: mean recovery = 104.4 %; coefficient of variation = 18.9 %
- Polyester strings: mean recovery = 70.5 %; coefficient of variation = 24.3 %
- Coverall sections: mean recovery = 100.8 %, coefficient of variation = 29.0 %
- Cotton wool filters: mean recovery = 105.6 %, coefficient of variation = 23.1 %

Based on the provisions of the OECD regarding occupational exposure to pesticides (OECD, 1997), airborne drift data were corrected for field recoveries.

3.4.3. *Airborne drift*

The results of the airborne drift measurements, corrected for a mean field recovery of 70.5 %, are shown in Fig. 5. For a given UAV sprayer, airborne drift generally increased with mean crosswind speed. Few exceptions from this general trend were observed, likely due to temporal and/or local wind fluctuations. With respect to the T30, airborne drift was observed to steadily decrease at increasing sampling height. Interestingly, this was not the case in 3 out of 4 trials performed with the T50, where the maximum amount of drift was observed at a sampling height of 2–3 m. The drift profiles produced by the P100 Pro were similar to those of the T30 in shape. However, substantially less tracer was recovered, even at mean crosswind speeds exceeding 5 m/s (trial 7).

3.4.4. *Ground deposition*

Ground deposition patterns inside and outside the target area for spraying are depicted in Fig. 6. Mean deposition inside the target area ranged from 22 to 95 % of the respective actual application rate. Deposition levels decreased with increasing downwind distances and were consistently below 1 % at a downwind distance of 50 m. Interestingly, mean deposition levels at a downwind distance of 1 m were similar to those inside the target area for trials 2, 4, 5, 7 and 9. These

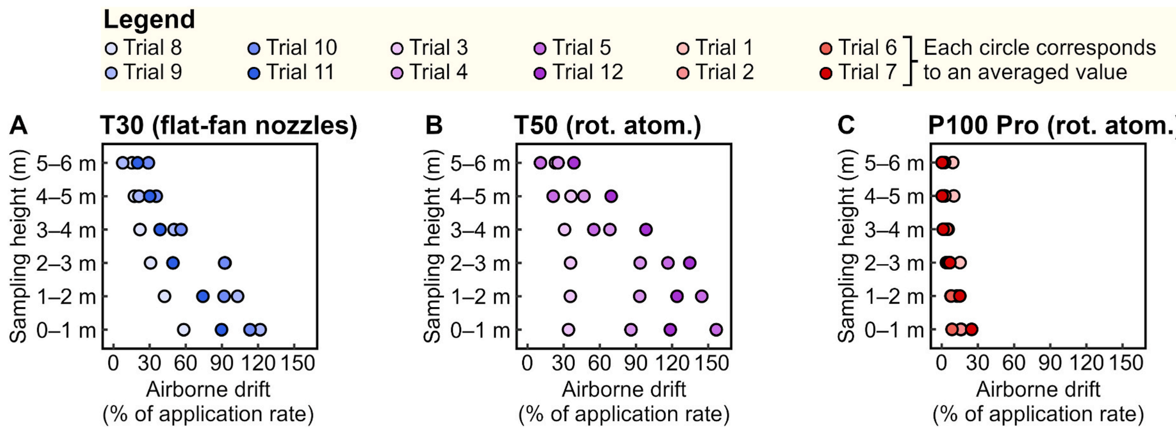

Fig. 5. Mean airborne drift at a downwind distance of 5 m corrected for field recoveries (Section 3.4.2). A-C. Results of trials involving the T30, T50 or P100 Pro, respectively.

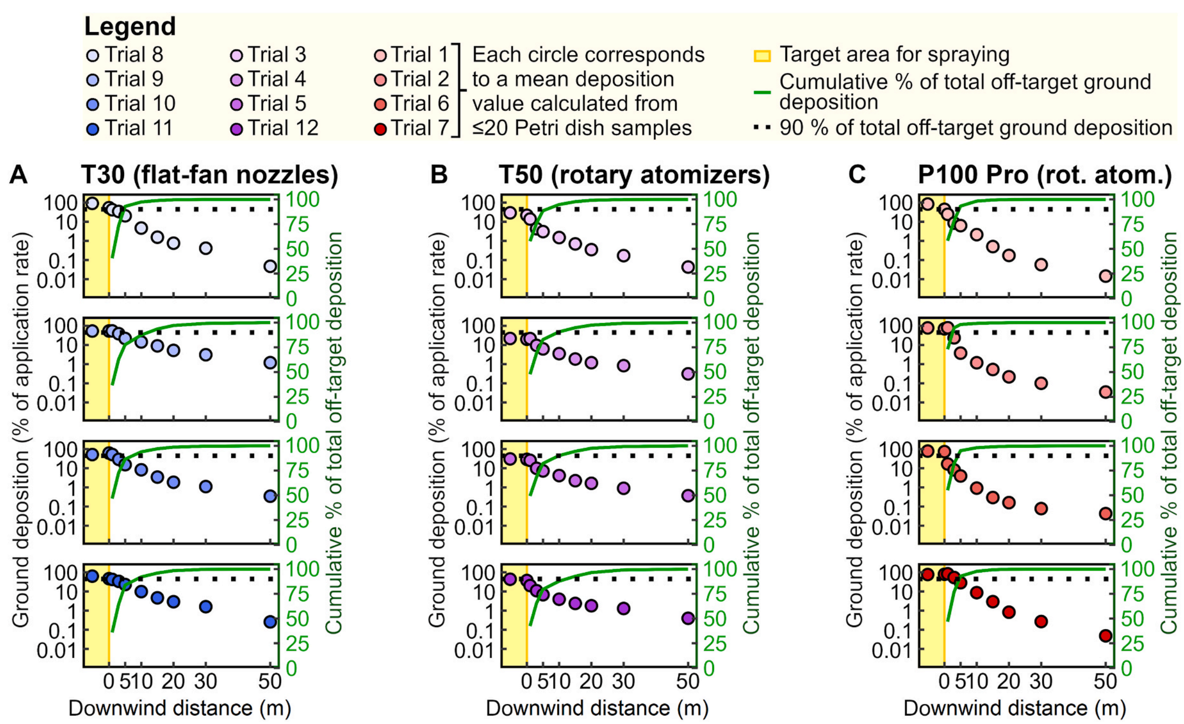

Fig. 6. Mean ground deposition up- and downwind of the edge of the target area. A-C. Results of trials involving the T30, T50 or P100 Pro, respectively. In all plots, the cumulative percentage of the total measured deposition downwind the target area is indicated (solid green line). The 90 % threshold is also represented (dotted line). (For interpretation of the references to colour in this figure legend, the reader is referred to the Web version of this article.)

trials were characterized by mean crosswind speeds ≥3 m/s, and hence, the observation is likely due to a downwind shift of the swath position. Cumulative projections were calculated for all datasets as described (see Fig. 6) (ISO 22866, 2005). For all trials, 90 % of the total amount of off-target deposition was observed within less than 15 m downwind of the edge of the target area. For the P100 Pro, the 90 % threshold was consistently reached at a downwind distance of less than 5 m.

Aggregate sub datasets were generated. They consisted of at least 73 individual deposition values per downwind distance and UAV sprayer. As illustrated in Fig. 7, individual values of a given sub dataset not only covered a wide range but were also often irregularly distributed. In general, dispersion was greatest in trials characterized by strong crosswind. Arithmetic means as well as 50th, 77th and 90th percentiles were computed for each sub dataset (Supplementary Table S4). These statistical descriptors were used to compare the off-target deposition levels caused by the three UAV sprayers under the experimental conditions. Except for the 50th drift percentile relating to a downwind distance of 50 m, all statistical descriptors derived for the T50 were below the respective descriptors computed for the T30. This suggests that the T50 produced less off-target ground deposit than the T30 under the experimental conditions tested. At downwind distances of 15 m and more, the P100 Pro produced less ground deposit than the other two UAV sprayers. However, comparatively high deposition levels were observed 1 m downwind, likely due to a shift of the swath position in trials 2 and 7 (see above). The comparison is illustrated in Supplementary Fig. S3A–C.

3.4.5. *Direct resident and bystander exposure to spray drift*

The drift trials involved display mannequins dressed in coveralls. For each mannequin used in a specific trial, the most exposed body part was determined. UAV-specific exposure patterns were not noted. At a

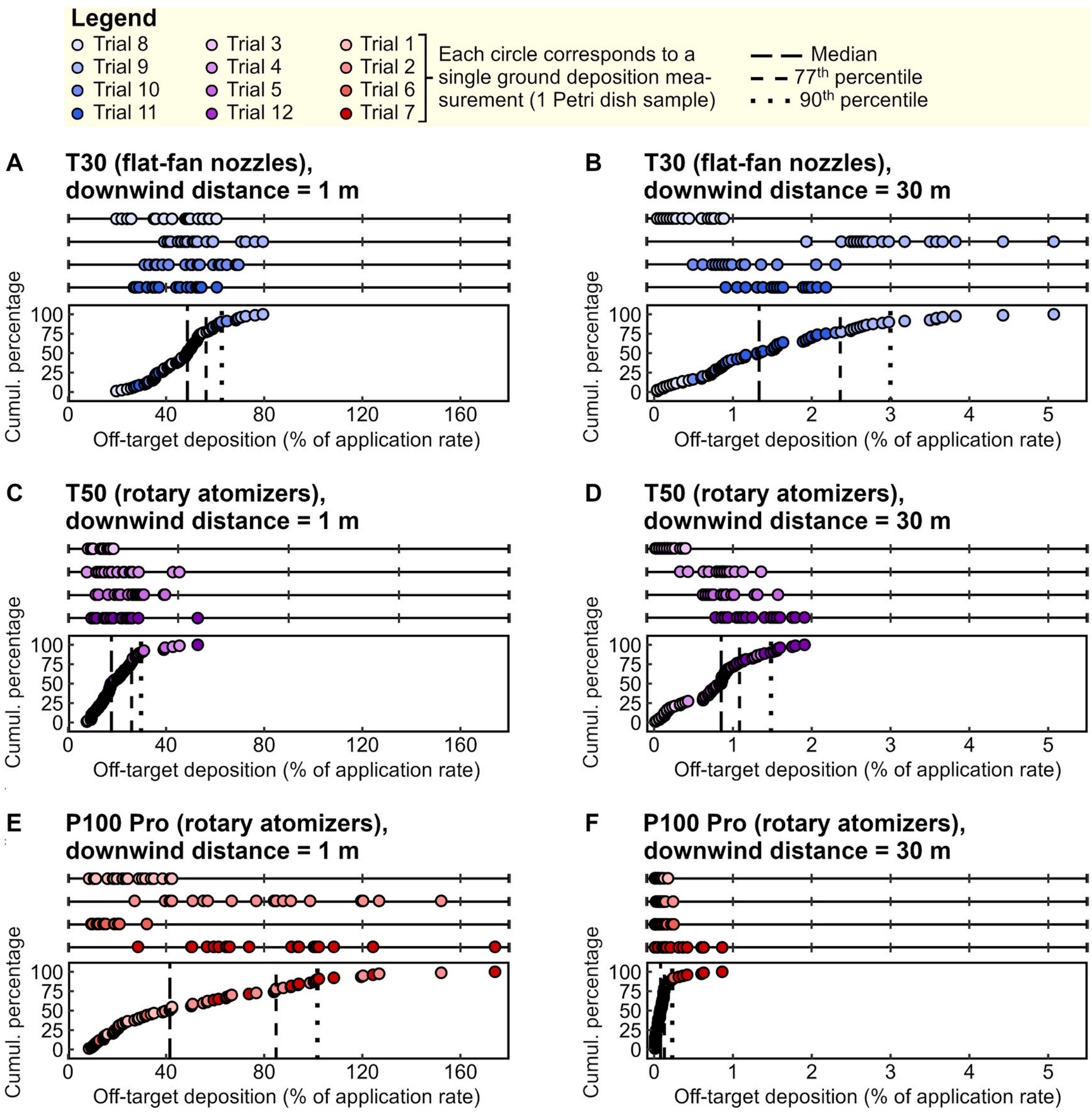

Fig. 7. Cumulative percentage graphs of selected ground deposition data. A-F. Results of trials involving the T30, T50 or P100 Pro, respectively. 1D plots illustrate the distribution of values observed within the same trial. Panels on the left relate to a downwind distance of 1 m while those on the right concern a downwind distance of 30 m.

downwind distance of 5 m, the most exposed body part of adult mannequins corresponded to the lower limbs in 30 out of 36 instances (Fig. 8, cartoons). With respect to child mannequins positioned at that downwind distance, the greatest amount of spray liquid impinged on the torso, the upper limbs or the lower limbs with 19, 14 and 3 instances, respectively. At greater downwind distances and independent of the mannequin type, the upper limbs or the torso were often the most exposed regions. These trends can be in part explained by relative sampling surface areas (adult mannequins: torso ~ lower limbs > upper limbs > head; child mannequins: torso > lower limbs > upper limbs > head).

Total potential dermal exposure values were calculated for each mannequin used in a specific trial as the total amount of tracer recovered from all coverall parts and expressed as volume of spray liquid. Sub datasets of total potential dermal exposure values relating to a specific UAV sprayer, downwind distance and mannequin type were generated and empirically described as log-normal distributions (EFSA PPR panel, 2010). Arithmetic means as well as 50th, 75th and 95th percentiles were computed from each sub dataset. Representative distributions of total potential dermal exposure levels, log-normal fits and selected statistical descriptors are shown in Fig. 8. Similar analyses were performed with respect to the potential dermal exposure of different body parts as well as the inhalation exposure data. Overall, both potential dermal and inhalation exposure values covered a wide range with the latter being substantially lower. Adult and child mannequins were not characterized by marked differences in total potential dermal exposure. The analyses did, however, confirm the preferential exposure patterns described in the previous paragraph. All statistical descriptors are given in Supplementary Table S5.

The exposure data collected were scaled to a spray volume of 100 L/ha, followed by generating sub datasets relating to a specific UAV sprayer, downwind distance and mannequin type. The arithmetic mean as well as 50th, 75th and 95th percentiles were computed for each sub dataset. These statistical descriptors were used to compare the exposure caused by the three UAV sprayers under the experimental conditions. At a downwind distance of 5 m, potential dermal exposure estimates followed the order T30 > P100 Pro ~ T50. The order T30 > T50 > P100 Pro was observed at greater downwind distances. As for inhalation exposure, the order T30 ~ T50 > P100 Pro was frequently observed across all downwind distances sampled. These trends are illustrated in Supplementary Fig. S3D–F. Overall, they are consistent with those observed for off-target ground deposition described in Section 3.4.4.

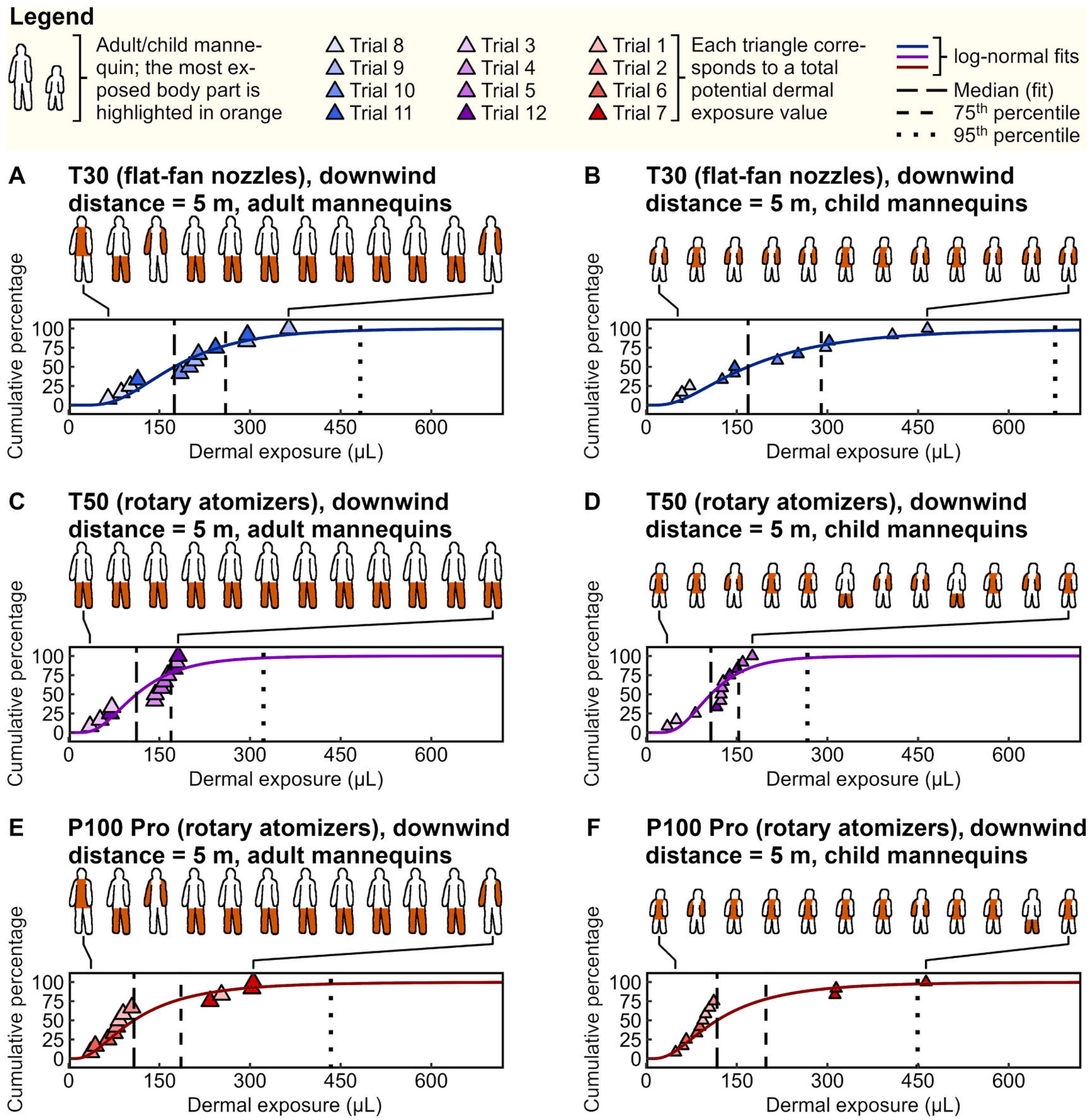

Fig. 8. Cumulative percentage graphs of total potential dermal exposure data. A-F. Results of trials involving the T30, T50 or P100 Pro, respectively. All panels relate to a downwind distance of 5 m. Panels on the left relate to adult mannequins while those on the right concern child mannequins. Solid lines correspond to cumulative representations of log-normal fits. As described in Section 2.7.3, each 75th and 95th percentile was computed from the respective fit function and statistically estimated. Only the higher of the two estimates is shown. Cartoons of mannequins were taken from Dubuis et al. (2023). For each mannequin, the most exposed body part is highlighted.

4. Discussion

It has been hypothesized that UAVs equipped with rotary atomizers may be associated with significant drift risk (Chen et al., 2022; Wang et al., 2020, 2023b). However, the rotary atomizers and hydraulic flat-fan nozzles tested here were not characterized by substantial differences with respect to the %V < 100 μm for a given $D_{V0.5}$. The underlying measurements were performed in a laboratory setting. Under field conditions, the two UAV sprayers equipped with rotary atomizers only occasionally produced more airborne drift and off-target ground deposition than the reference UAV sprayer fitted with hydraulic flat-fan nozzles. Similar observations were made with respect to direct resident/bystander exposure to spray drift. The combined results do not suggest that the delivery system is a key driver of drift. Along these lines, a DJI Agras T25, which is equipped with rotary atomizers, has recently been shown to produce similar or lower drift levels than a DJI Agras T30 equipped with hydraulic air-induction nozzles under typical use conditions (Ahrens et al., 2025).

The following drivers of off-target droplet movement were identified in the drift and exposure trials performed herein:

- Crosswind: For a given UAV sprayer, drift and resident/bystander exposure generally increased at greater crosswind speeds. In addition, the ground deposition data revealed swath off-setting at mean crosswind speeds ≥3 m/s.
- Droplet size: Comparison of the drift and resident/bystander exposure levels observed for the T30/T50 with those observed for the P100 Pro suggests that the droplet size has a substantial influence on off-target droplet movement.

Both crosswind and droplet size have previously been identified as sensitive parameters in the context of off-target movement in UAV-based plant protection treatments (Bonds et al., 2023, 2024; Dubuis et al., 2023). Further parameters may have influenced the outcome of the drift and exposure trials: For example, the T50 weighed 92 kg at the beginning of the application while the T30 weighed only 66.5 kg. Less weight is associated with decreased downwash, and hence, a decreased ability to draw droplets to the ground (Chen et al., 2022). This could have contributed to the observation that the T30 was generally characterized by higher drift and exposure levels than the T50. Differences with respect to temperature, relative humidity, UAV rotor configuration and/or nozzle/atomizer layout may have further influenced the results of the field trials (Bonds et al., 2024; Zhang et al., 2023).

For applications made during crosswind, the FAO/WHO recommend compensating for the swath displacement by adjusting the path of the aircraft upwind of the downwind edge of the field (FAO & WHO, 2024). While this was not within the scope of the present study, adjusting the flight lines accordingly could have been used to prevent swath displacement beyond the edge of the target area in the drift and exposure trials. Automatic flight line adjustments based on real-time ambient wind data may be technically feasible in the future to further optimize deposition within the target zone and reduce off-target losses (Bonds et al., 2023; Portillo et al., 2025). The FAO/WHO further state that drift from aerial spraying can be effectively reduced by applying the largest droplets that provide sufficient coverage and control (FAO & WHO, 2024). A future direction for balancing drift risk and coverage of UAV sprayers equipped with rotary atomizers could be to dynamically adapt the spray quality in-flight by adjusting disc speeds. Such dynamic droplet-size control has recently been described (Chen et al., 2026). The development of a standardized droplet sizing protocol for rotary atomizers, which was previously proposed by others (Ahrens et al., 2025), would help harnessing the full potential of dynamic droplet-size control. Further measures exist to reduce the drift risk associated with UAV-based plant protection treatments. These include, for example, a reduction in flight speed and flight height (Goulet-Fortin et al., 2024; Li et al., 2021; Zhang et al., 2023).

For a meaningful risk-benefit analysis, it is crucial to compare the risks of UAV sprayers against those of other application equipment. In this context, ground boom sprayers constitute an important reference due to their widespread use. In the European Union, reference drift curves are used to predict the environmental concentration of pesticides in surface waters following treatments with ground boom sprayers (FOCUS, 2001). These curves relate to trials involving field crops and hydraulic nozzles producing “medium” spray (Ganzelmeier et al., 1995; Rautmann et al., 2001). Similar reference drift curves have also been implemented in the AgDRIFT model (Teske et al., 2002), which is used by the US EPA for terrestrial and aquatic assessments (US EPA et al., 2013). AgDRIFT also permits to estimate drift from aerial applications. Spray qualities that are available in AgDRIFT include “fine to medium/coarse” and “very fine to fine” (both tier I ground) as well as “fine to medium” (tier I aerial) (Teske et al., 2002; US EPA et al., 2013).

The ground deposition data collected in the present study were compared against reference curves from the EU and US. Here, the statistical descriptors used for comparison were calculated from the entire dataset, *i.e.*, they relate to UAVs fitted with different spraying systems. The comparison suggests that off-target deposition from UAV sprayers is likely less than that produced by manned aircrafts and more than that of ground boom sprayers (Fig. 9A–C). This finding corroborates the results of earlier comparisons (Bonds et al., 2024; Goulet-Fortin et al., 2024). Interestingly, the off-target deposition data collected herein matched well with the AgDRIFT reference dataset relating to ground boom sprayers producing “very fine” droplets (Fig. 9D).

Finally, the results of the present study were compared to the reference values used to estimate resident/bystander exposure in the context of the European risk assessment process (EFSA, 2022). In the corresponding model, several exposure pathways are considered, two of

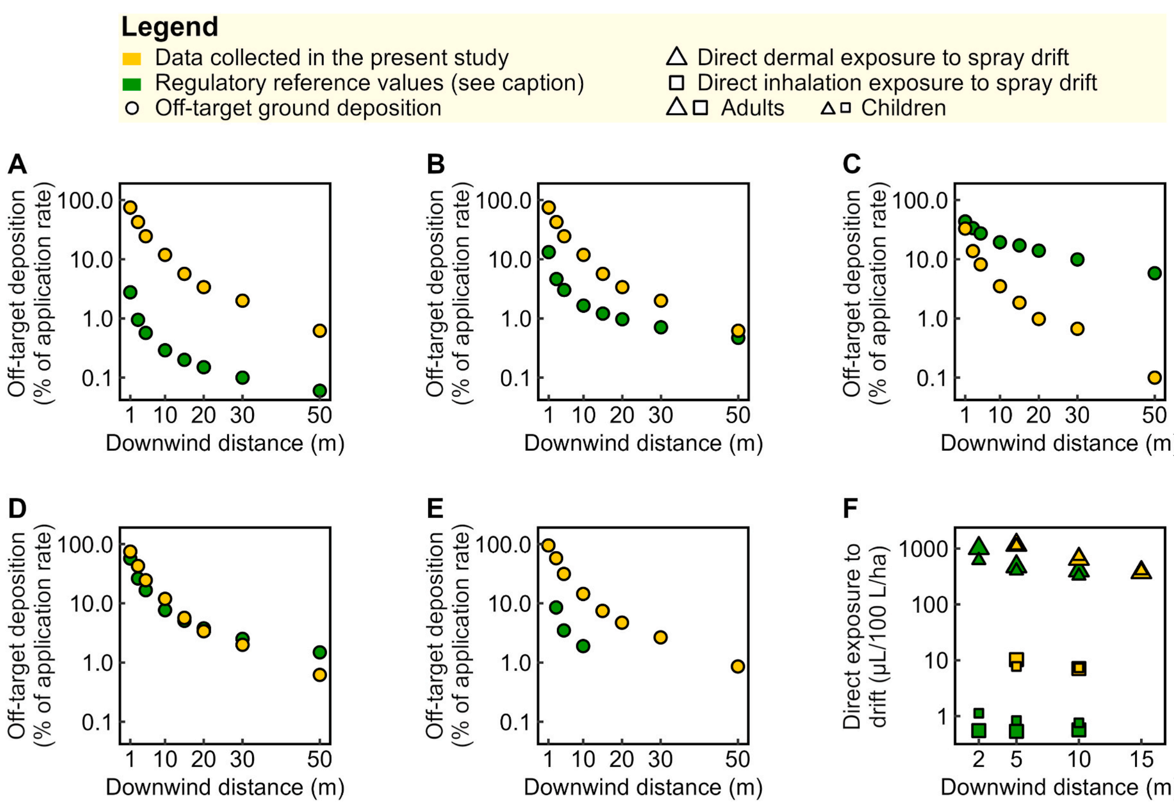

Fig. 9. Comparison of the ground deposition and exposure data collected in the present study against different regulatory reference datasets as indicated. A. Rautmann et al. (2001), field crops, 90th percentiles. B. AgDRIFT, boom sprayer, high boom, fine-medium/coarse droplets, 90th percentiles. C. AgDRIFT, tier I aerial, fine-medium droplets. D. AgDRIFT, boom sprayer, high boom, very fine droplets, 90th percentiles. E. EFSA (2022), field crops, “surface deposit”, 95th percentiles. F. EFSA (2022), field crops, “spray drift”, 95th percentiles. Ground deposition and exposure percentiles derived from the UAV data set correspond to n^{th} percentile values, where n was generally chosen to match the percentile of the reference. For comparison with the tier I aerial drift data represented in panel C, 50th percentiles were selected.

which a drift-related: Indirect exposure due to off-target ground deposition and direct exposure to spray drift (EFSA, 2022). In the present work, the reference values relating to direct exposure to spray drift were scaled to a spray volume of 100 L/ha. Subsequently, statistical descriptors scaled to the same spray volume were calculated from the present dataset. Here, total potential dermal exposure estimates were converted into actual exposure estimates by assuming that the exposure of the torso corresponds to 50 % of its potential exposure. An analogous adjustment is made in the regulatory model (EFSA, 2022). All estimates relating to UAV-based treatments were found to be higher than the corresponding reference values for ground boom sprayers (Fig. 9E and F). This result supports the findings described in the previous paragraph. It is noteworthy that numerous reference values relating to the drift potential of ground boom sprayers can be matched with the data of the present study by setting off the reference curve along the x-axis. This suggests that the two application techniques can be characterized by a similar drift risk if UAV sprayers respect an additional unsprayed buffer zone.

5. Conclusion

This work addressed environmental, resident and bystander exposure resulting from plant protection treatments with a reference UAV sprayer fitted with hydraulic flat-fan nozzles as well as two UAV sprayers equipped with rotary atomizers. Overall, crosswind and droplet size rather than the delivery system were identified as primary drivers of off-target droplet movement. These findings are anticipated to be useful in a regulatory context. Given the sensitivity of the drift risk to the droplet size, dynamic droplet-size control is considered an interesting approach to balancing drift risk and coverage. It would benefit from the development of a standardized droplet sizing protocol for rotary atomizers. The methodology used in the present study may be helpful in this context. The present dataset also highlights the potential of flight line adjustments to prevent crosswind-driven swath off-setting beyond the edge of the target area. Finally, a comparative assessment of the data collected in the present study with various regulatory reference datasets confirmed that spray drift of UAV sprayers is likely less than that of manned aircrafts but more than that of ground boom sprayers. However, a ground boom sprayer and a UAV sprayer might be characterized by similar drift risk under certain circumstances, especially when the ground boom sprayer generates a higher fraction of drift-prone droplets and/or the size of the unsprayed buffer zone for the UAV sprayer is higher.

Funding

This research did not receive any specific grant from funding agencies in the public, commercial, or not-for-profit sectors.

CRediT authorship contribution statement

Pierre-Henri Dubuis: Conceptualization, Data curation, Investigation, Methodology, Project administration, Resources, Supervision, Writing – review & editing. **Céline Villars-Corbex:** Data curation, Investigation, Methodology, Validation, Writing – review & editing. **M. Clare Butler Ellis:** Methodology. **H. Christoph Geiser:** Writing – review & editing. **Jeremy J. Harwood:** Project administration, Resources, Writing – review & editing. **Marco C. Knobloch:** Writing – review & editing. **Andrew G. Lane:** Investigation, Methodology, Validation. **Aurélie Melgar:** Investigation, Validation. **Joel D. Stohler:** Investigation, Methodology, Resources, Validation, Writing – review & editing. **Clive R. Tuck:** Data curation, Formal analysis. **Helen C. Wheeler:** Investigation, Methodology, Validation. **Jürg A. Zarn:** Conceptualization, Writing – review & editing. **Sebastian L.B. König:** Conceptualization, Data curation, Formal analysis, Investigation, Methodology, Project administration, Supervision, Visualization, Writing – original draft.

Declaration of competing interest

The authors declare that they have no known competing financial interests or personal relationships that could have appeared to influence the work reported in this paper.

Acknowledgements

The authors thank AutoSpray Systems Ltd, Da-Jiang Innovations Science and Technology Co., Ltd, DigitalRoots SA and Sky53 sagl for their support regarding the UAV sprayers tested. Regarding the field trials, the authors thank David Knecht and Lattion-Ruppen Association by Pascal Lattion for the permission to use their plots as trial sites. Numerous employees of Agroscope, the Federal Office for Civil Aviation and the State Secretariat for Economic Affairs helped with the field work. Their help is gratefully acknowledged. Photographs used in the present work were taken by employees of Agroscope Changins, the Federal Food Safety and Veterinary Office and the Silsoe Spray Applications Unit. Commercial trade and product names are exclusively used for clarity, not to make any implicit endorsements.

Appendix A. Supplementary data

Supplementary data to this article can be found online at https://doi.org/10.1016/j.cropro.2026.107776.

Data availability

Data will be made available on request.

References

Ahmad, F., Zhang, S., Qiu, B., Ma, J., Xin, H., Qiu, W., Ahmed, S., Chandio, F.A., Khaliq, A., 2022. Comparison of water sensitive paper and glass strip sampling approaches to access spray deposit by UAV sprayers. Agronomy 12, 1302.
Ahrens, K., Herbst, A., Wegener, J.K., 2025. Field comparison of spray drift from unmanned aerial spraying systems using air-induction nozzles versus rotary atomizers. Front. Agron. 7, 1716113.
Anken, T., Coupy, G., Dubuis, P.-H., Favre, G., Geiser, H.C., Gurba, A., Häni, M., Hochstrasser, M., Landis, M., Maitre, T., Moor, C., Mouron, P., Sanvido, O., Wagner, Y., Zarn, J.A., König, S.L.B., 2025. Plant protection treatments in Switzerland using unmanned aerial vehicles: regulatory framework and lessons learned. Pest Manag. Sci. 81, 3419–3429.
Bonds, J.A.S., Fritz, B., Thistle, H.W., 2023. Calculation of swath width and swath displacement for uncrewed aerial spray systems. J. ASABE 66, 523–532.
Bonds, J.A.S., Pai, N., Hovinga, S., Stump, K., Haynie, R., Flack, S., Bui, T., 2024. Spray drift, operator exposure, crop residue and efficacy: early indications for equivalency of uncrewed aerial spray systems with conventional application techniques. Journal ASABE 67, 27–41.
Brown, C.R., Giles, D.K., 2018. Measurement of pesticide drift from unmanned aerial vehicle application to a vineyard. Trans. ASABE 61, 1539–1546.
Butler Ellis, M.C., Lane, A.G., O'Sullivan, C.M., Wheeler, H.C., Harwood, J.J., 2026. Field measurement of spray drift from a spray application by UAV. Pest Manag. Sci. 82, 7225–7234. https://doi.org/10.1002/ps.8645.
Castro-Tenzi, S., Winchell, M., Tang, Z., Teske, M.E., Whitehouse, G.R., Fritz, B., Martin, D., 2025. Validation of the spray drift modeling software AGDISPpro applied to remotely piloted aerial application systems. Sci. Total Environ. 966, 178725.
Chen, P., Douzals, J.P., Lan, Y., Cotteux, E., Delpuech, X., Pouxviel, G., Zhan, Y., 2022. Characteristics of unmanned aerial spraying systems and related spray drift. Front. Plant Sci. 13, 870956.
Chen, P., Wu, J., Bian, Z., Douzals, J.P., Qin, Y., Liu, H., Wang, J., Lan, Y., 2026. Optimization of spraying quality and drift risk in unmanned aerial spraying systems (UASS) based on Multi-Gradient droplet size control. Comput. Electron. Agric. 244, 111481.
Chen, S., Lan, Y., Zhou, Z., Ouyang, F., Wang, G., Huang, X., Deng, X., Cheng, S., 2020. Effect of droplet size parameters on droplet deposition and drift of aerial spraying by using plant protection UAV. Agronomy 10, 195.
Dubuis, P.-H., Droz, M., Melgar, A., Zürcher, U.A., Zarn, J.A., Gindro, K., König, S.L.B., 2023. Environmental, bystander and resident exposure from orchard applications

using an agricultural unmanned aerial spraying system. Sci. Total Environ. 881, 163371.
EFSA, 2022. Guidance on the assessment of exposure of operators, workers, residents and bystanders in risk assessment of plant protection products. EFSA J. 20, 7032.
EFSA PPR panel, 2010. Scientific opinion on preparation of a guidance document on pesticide exposure assessment for workers, operators, bystanders and residents. EFSA J. 8, 1501.
FAO & WHO, 2024. International Code of Conduct on Pesticide Management – Guidance for Aerial Application of Pesticides. https://doi.org/10.4060/cc8321en. Rome.
FOCUS, 2001. FOCUS Surface Water Scenarios in the EU Evaluation Process Under 91/414/EEC, SANCO/4802/2001-rev.2 Final (May 2003).
Fritz, B.K., Martin, D.E., 2020. Measurement and analysis methods for determination of effective swath width from unmanned aerial vehicles. In: Elsik, C.M. (Ed.), Proceedings of the Pesticide Formulation and Delivery Systems: 40th Volume, Formulation, Application, and Adjuvant Innovation, 2020, West Conshohocken, PA. https://doi.org/10.1520/STP162720190132.
Ganzelmeier, H., Rautmann, D., Spangenberg, R., Streloke, M., 1995. Studies on the spray drift of plant protection products. Mitteilungen aus der BBA für Land- und Forstwirtschaft Berlin-Dahlem 305, 1–110.
Gao, B., Sasturain, J., Wiemann, C., Hewitt, N.J., Gan, W.J., Wang, G., Lan, Y., Blaschke, U., 2025. Measurement of bystander dermal exposure resulting from drift after drone application under three crop treatment scenarios. ACS Agric Sci. Technol. 5 (4), 542-542.
Glass, C.R., 2006. Field Study methods for the determination of bystander exposure to pesticides. In: Martínez Vidal, J.L., Frenich, A.G. (Eds.), Pesticide Protocols. Humana Press, Totowa, NJ, pp. 165–177. https://doi.org/10.1385/1-59259-929-x:165.
Goulet-Fortin, J., He, Q., Donaldson, F., Gottesbueren, B., Wang, G., Lan, Y., Gao, B., Gan, W.J., Jiang, Y.N., Laabs, V., 2024. Evaluating spray drift from Uncrewed Aerial Spray Systems: a machine learning and variance-based sensitivity analysis of environmental and spray system parameters. Sci. Total Environ. 934, 173213.
Herbst, A., Bonds, J., Wang, Z., Zeng, A., He, X., Goff, P., 2020. The influence of unmanned agricultural aircraft system design on spray drift. Journal für Kulturpflanzen 72, 1–11.
Huang, Z., Wang, C., Li, Y., Zhang, H., Zeng, A., He, X., 2023a. Field evaluation of spray drift and nontargeted soybean injury from unmanned aerial spraying system herbicide application under acceptable operation conditions. Pest Manag. Sci. 79, 1140–1153.
Huang, Z., Wang, C., Wongsuk, S., Qi, P., Liu, L., Qiao, B., Zhong, L., He, X., 2023b. Field evaluation of a six-rotor unmanned agricultural aerial sprayer: effects of application parameters on spray deposition and control efficacy against rice planthopper. Pest Manag. Sci. 79, 4664–4678.
ISO 22866, 2005. Equipment for Crop Protection — Methods for Field Measurement of Spray Drift.
ISO 25358, 2018. Crop Protection Equipment — Droplet-size Spectra from Atomizers — Measurement and Classification.
Kassambara, A., 2025. Ggpubr: 'ggplot2' based publication ready plots. https://rpkgs.datanovia.com/ggpubr/.
Lan, X., Wang, J., Chen, P., Liang, Q., Zhang, L., Ma, C., 2024. Risk assessment of environmental and bystander exposure from agricultural unmanned aerial vehicle sprayers in golden coconut plantations: effects of droplet size and spray volume. Ecotoxicol. Environ. Saf. 282, 116675.
Li, X., Giles, D.K., Andaloro, J.T., Long, R., Lang, E.B., Watson, L.J., Quandah, I., 2021. Comparison of UAV and fixed-wing aerial application for alfalfa insect pest control: evaluating efficacy, residues, and spray quality. Pest Manag. Sci. 77, 4980–4992.
Liu, Y., Li, L., Liu, Y., He, X., Song, J., Zeng, A., Wang, Z., 2020. Assessment of spray deposition and losses in an apple orchard with an unmanned agricultural aircraft system in China. Trans. ASABE 63, 619–627.
Murphy, S.D., Nicholls, T., Whybrew, A., Tuck, C.R., Parkin, C.S., 2001. Classification and imaging of agricultural sprays using a particle/droplet image analyser. In: Proceedings of the BCPC Conference Weeds, 2001. Brighton.
OECD, 1997. Guidance document for the conduct of studies of occupational exposure to pesticides during agricultural application. Series on Testing and Assessment. No. 9.
OECD, 2021. Report on the state of the knowledge – literature review on unmanned aerial spray systems in agriculture. OECD Series on Pesticides. OECD Publishing, Paris, France.
Portillo, H., Barbosa, R., Beckwith, M., Gullen, T., Haynie, R., Hovinga, S., Kesavaraju, B., Lang, E., Livingston, P., Newton, N., Oostlander, M., Watson, G., Sinha, R., 2025. Industry (UAPASTF) response to pesticide regulators' "State of the Knowledge" review of drone use for pesticide application: best practices for safe and effective application of pesticides. Drones 9, 388.
Psiroukis, V., Kasimati, A., Nychas, K., Anastasiou, E., Balafoutis, A., Fountas, S., 2026. Comparison of spray drift between spraying drone and conventional airblast sprayer in vineyards. Smart Agr. Tech 13, 101741.
Rautmann, D., Streloke, M., Winkler, R., 2001. New basic drift values in the authorisation procedure for plant protection products. Mitteilungen aus der Biologischen Bundesanstalt für Land- und Forstwirtschaft (Federal Biological Research Center for Agriculture and Forestry), pp. 133–141. Berlin, Germany.
Shan, C., Wu, J., Song, C., Chen, S., Wang, J., Wang, H., Wang, G., Lan, Y., 2022. Control efficacy and deposition characteristics of an unmanned aerial spray system low-volume application on corn fall armyworm *Spodoptera frugiperda*. Front. Plant Sci. 13, 900939.
Sánchez-Fernández, L., Barrera, M., Martínez-Guanter, J., Pérez-Ruiz, M., 2023. Drift reduction in orchards through the use of an autonomous UAV system. Comput. Electron. Agric. 211, 107981.
Sánchez-Fernández, L., Barrera-Baéz, M., Martínez-Guanter, J., Pérez-Ruiz, M., 2024. Reducing environmental exposure to PPPs in super-high density olive orchards using UAV sprayers. Front. Plant Sci. 14, 1272372.
Sánchez-Fernández, L., Díaz-García, F., Pérez-Ruiz, M., Sandin-España, P., Alonso-Prados, J.L., Mateo-Miranda, M., Martínez-Guanter, J., García-Montero, E., del Carmen Márquez, M., Abril-Muñoz, I., 2025. Dermal exposure of operators, bystanders and residents derived from unmanned aerial spraying systems (UASS) in vineyard. Drones 9, 345.
Teske, M.E., Bird, S.L., Esterly, D.M., Curbishley, T.B., Ray, S.L., Perry, S.G., 2002. AgDrift®: a model for estimating near-field spray drift from aerial applications. Environ. Toxicol. Chem. 21, 659–671.
US EPA, 2026. Introduction to pesticide drift. available online: https://www.epa.gov/reducing-pesticide-drift/introduction-pesticide-drift. (Accessed 15 June 2026).
US EPA, White, K., Khan, F., Peck, C., Corbin, M., 2013. Guidance on Modeling Offsite Deposition of Pesticides via Spray Drift for Ecological and Drinking Water Assessments (Draft for Comment).
Venables, W.N., Ripley, B.D., 2002. Modern Applied Statistics with S, fourth ed. Springer, New York.
Wang, C., Herbst, A., Zeng, A., Wongsuk, S., Qiao, B., Qi, P., Bonds, J., Overbeck, V., Yang, Y., Gao, W., He, X., 2021. Assessment of spray deposition, drift and mass balance from unmanned aerial vehicle sprayer using an artificial vineyard. Sci. Total Environ. 777, 146181.
Wang, C., Wongsuk, S., Huang, Z., Yu, C., Han, L., Zhang, J., Sun, W., Zeng, A., He, X., 2023a. Comparison between drift test bench and other techniques in spray drift evaluation of an eight-rotor unmanned aerial spraying system: the influence of meteorological parameters and nozzle types. Agronomy 13, 270.
Wang, G., Han, Y., Li, X., Andaloro, J., Chen, P., Hoffmann, W.C., Han, X., Chen, S., Lan, Y., 2020. Field evaluation of spray drift and environmental impact using an agricultural Unmanned Aerial Vehicle (UAV) sprayer. Sci. Total Environ. 737, 139793.
Wang, G., Lan, Y., Qi, H., Chen, P., Hewitt, A., Han, Y., 2019. Field evaluation of an unmanned aerial vehicle (UAV) sprayer: effect of spray volume on deposition and the control of pests and disease in wheat. Pest Manag. Sci. 75, 1546–1555.
Wang, G., Zhang, T., Song, C., Yu, X., Shan, C., Gu, H., Lan, Y., 2023b. Evaluation of spray drift of plant protection drone nozzles based on wind tunnel test. Agronomy 13, 628.
Wang, X., He, X., Song, J., Wang, Z., Wang, C., Wang, S., Wu, R., Meng, Y., 2018. Drift potential of UAV with adjuvants in aerial applications. Int. J. Agric. Biol. Eng. 11, 54–58.
Wang, X., Zhang, Y., Hu, H., Liu, B., Wang, F., Zhang, Y., Wang, W., Li, X., Xu, W., 2023c. Evaluation of the droplet deposition and control effect of a special adjuvant for unmanned aerial vehicle (UAV) sprayers. J. Pestic. Sci. 48, 78–85.
Wickham, H., 2016. ggplot2: Elegant Graphics for Data Analysis, second ed. Springer-Verlag, New York.
Xue, X.Y., Kang, Tu, Qin, W.C., Lan, Y.B., Zhang, H.H., 2014. Drift and deposition of ultra-low altitude and low volume application in paddy field. Int. J. Agric. Biol. Eng. 7, 23–28.
Zhang, R., Hewitt, A.J., Chen, L., Li, L., Tang, Q., 2023. Challenges and opportunities of unmanned aerial vehicles as a new tool for crop pest control. Pest Manag. Sci. 79, 4123–4131.